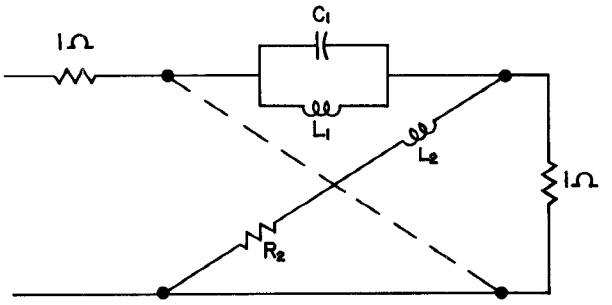

Fig. 3. The normalized lumped lattice network: $C_1 = 6.7517\omega_c^{-1}$ F, $L_1 = 0.0561\omega_c^{-1}$ H, $R_2 = 4\times10^{-5}\ \Omega$, and $L_2 = 0.0941\omega_c^{-1}$ H

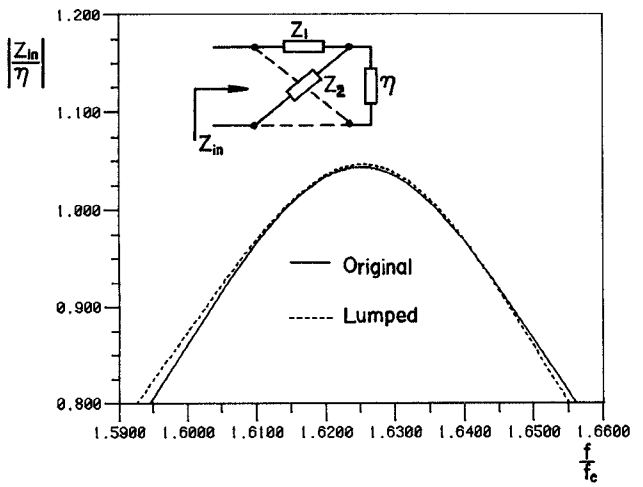

Fig. 4. The input impedance of the original network versus the input impedance of the lumped lattice network in the bandwidth.

where u is the unit impulse function, and the residue A is equal to the area under $R_1(\omega)$.

The reactance of the cross-arm impedance is clearly that of an inductor. Although sudden changes also occur in the resistive part of the cross arm, this cannot be attributed to the inductor. The value of the resistive part, however, is basically constant in the bandwidth except for this sudden change at resonance. Consequently, assuming small losses, the impedance of this arm can be realized in the bandwidth by an inductor in series with a resistor; viz.,

$$Z_2(\omega) \simeq R_2 + j\omega L_2. \tag{5}$$

The evaluation of the elements of the lumped lattice network is rather straightforward. First, the area under $R_1(\omega)$ is determined and assigned to the residue A. The capacitor C_1 is then found as

$$C_1 = \frac{\pi}{2A} \tag{6}$$

while the inductor L_1 is found from (3). Furthermore, the inductor L_2 of the cross arm is readily determined as the slope of $X_2(\omega)$, or more simply as

$$L_2 = \frac{X_2(\omega_0)}{\omega_0}. \tag{7}$$

Finally, the resistor R_2 is assigned the constant value it has in the bandwidth. The normalized lumped lattice network obtained is shown in Fig. 3. The input impedance of the developed lumped network is shown in Fig. 4, where it can be seen that it agrees rather well with the input impedance of the original network in the bandwidth. In passing, it is noted that other choices of R_2, such as $R_2(\omega_0)$ or the area under $R_2(\omega)$ in the bandwidth divided by the bandwidth, change very little of the input impedance of the lumped lattice network.

IV. Summary

It has been shown in this paper that the lattice network can be used to overcome the difficulties associated with the T network representation of symmetrical configurations of lossy dielectric posts in a rectangular waveguide. If resonant, a lattice network of lumped elements can be developed to approximately realize the impedance matrix of the posts in the bandwidth. This lumped representation is particularly useful in the design of microwave filters employing dielectric posts in a rectangular waveguide.

Acknowledgment

The authors gratefully acknowledge the helpful remarks from some of the reviewers.

References

[1] C-I G. Hsu and H. A. Auda, "Multiple dielectric posts in a rectangular waveguide," *IEEE Trans. Microwave Theory Tech.*, vol. MTT-34, pp. 883–891, Aug. 1986.

[2] C-I G. Hsu and H. A. Auda, "Multiple dielectric posts in a rectangular waveguide," *Tech. Rep.*, Department of Electrical Engineering, University of Mississippi, University, MS, Aug. 1986.

[3] C. G. Montgomery, R. H. Dicke, and E. M. Purcell, Eds., *Principles of Microwave Circuits*. New York: McGraw-Hill, 1950.

[4] D. Kajfez, *Notes on Microwave Circuits*, vol. 1, Kajfez Consulting, Oxford, MS, 1984.

[5] E. A. Guillemin, *Synthesis of Passive Networks*. New York: Wiley, 1957. Reprinted by Robert E. Krieger Publishing Company, Huntington, NY, 1977.

Attenuation Distortion of Transient Signals in Microstrip

TONY LEUNG, STUDENT MEMBER, IEEE, AND
CONSTANTINE A. BALANIS, FELLOW, IEEE

***Abstract*—Attenuation distortion, and combinations of dispersion and attenuation distortions, of transient signals in microstrip lines are investigated. Conduction losses are considered for the general case where the strip conductor resistivity is different from that of the ground plane. Dielectric losses are examined for commonly used isotropic substrates. Attenuation and dispersion distortions of short pulses are shown to vary as microstrip and pulse parameters are changed.**

I. Introduction

The analysis of transient signal behavior in microstrip lines is essential for the design of MIC's that operate at high switching speeds or high frequencies. This behavior has been investigated in the past only for the case of distortions due to dispersion [1]–[3]. Analyzing dispersion distortion is important because it signifi-

Manuscript received August 13, 1987; revised November 1, 1987. This work was supported in part by the U.S. Army Research Office under Contract DAAG29-85-K-0078.

T. Leung was with the Department of Electrical and Computer Engineering, Arizona State University, Tempe. He is now with the Aerospace Corporation, El Segundo, CA 90245

C. A. Balanis is with the Department of Electrical and Computer Engineering, Arizona State University, Tempe, AZ 85287.

IEEE Log Number 8719439

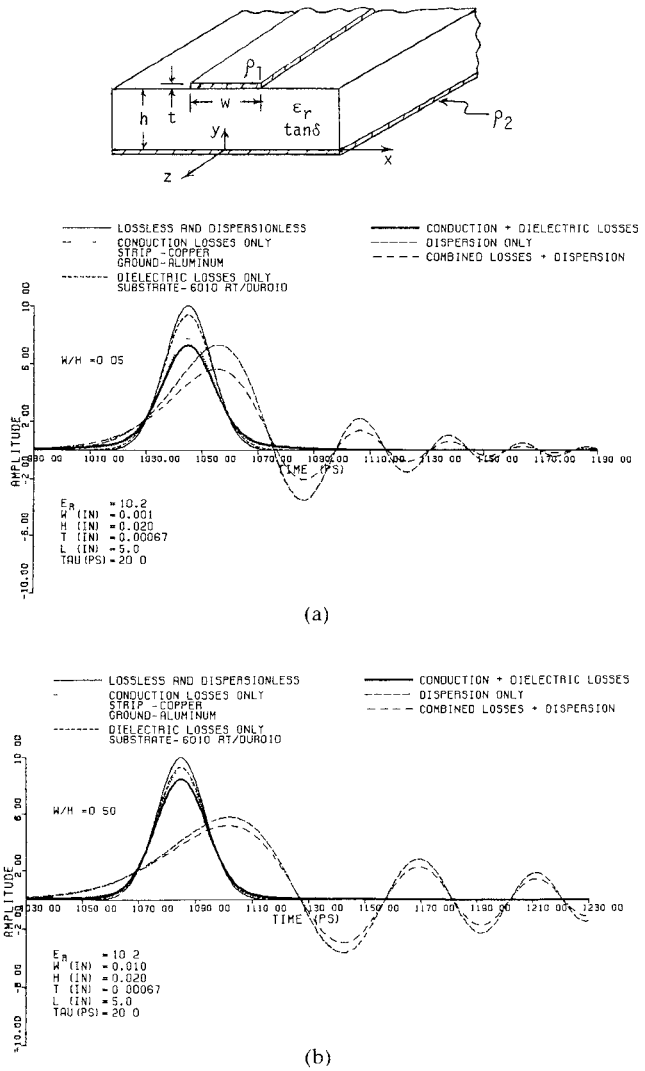

Fig 1. Gaussian pulse attenuation and dispersion as functions of strip width at $L = 5$ in (12.7 cm) along a microstrip line

cantly alters the form of a pulse as it propagates down the line. Similarly, attenuation distortion is vital because it also changes the form of a propagating pulse, but in a way different from dispersion distortion. Pulse distortion characteristics have been examined for waveguides and other guiding structures with dispersion and attenuation [4], [5]. For microstrip, however, attenuation distortion has not yet been examined.

This paper considers the attenuation distortion of short pulses propagating along microstrip lines. Attention is also given to dispersion distortion of pulses. The attenuation mechanisms here are due to conduction and dielectric losses. Radiation losses were not considered because they are significant only in microstrip lines with discontinuities [6]. Conduction losses are treated for cases where the strip conductor resistivity is different from that of the ground plane. The dielectric substrates considered here are isotropic materials with relatively high loss characteristics (such as duroids). Results show that the amount of pulse distortion (compared to distortionless pulses) varies as microstrip and pulse parameters change. Microstrip parameters include geometry dimensions (i.e., strip width and substrate height) and substrate dielectric constant (Fig. 1), whereas pulse parameters include pulse width (in picoseconds) and pulse rise time (pulse shape). The effect of the strip thickness is not shown here since it was found to have negligible significance in both attenuation and dispersion distortions (a constant strip thickness of 0.00067 in is used here, which is the thickness of 1/2 oz. copper).

II. Formulation

The attenuation constant for a continuous microstrip line can be written as [7] (assuming no radiation losses)

$$\alpha(\omega) = \alpha_c(\omega) + \alpha_d(\omega) \tag{1}$$

where $\alpha_c(\omega)$ and $\alpha_d(\omega)$ represent, respectively, the conduction and dielectric losses. If we assume that the surface resistivity of the strip conductor (R_{s1}) is different from the surface resistivity of the ground plane (R_{s2}) (which is common in many applications), then following the procedure in [8] and [9], $\alpha_c(\omega)$ can be expressed as

$\frac{w}{h} \leqslant \frac{1}{2\pi}$:

$$\alpha_c(\omega) = \frac{1}{2\pi Z_0 h}\left\{1-\left(\frac{w'}{4h}\right)^2\right\}\left\{\frac{R_{s1}+R_{s2}}{2} + R_{s1}\frac{h}{w'} \cdot\left[1+\frac{t}{\pi w}+\frac{1}{\pi}\ln\left(\frac{4\pi w}{t}\right)\right]\right\} \quad \left(\frac{\text{nepers}}{\text{unit length}}\right) \tag{2a}$$

$\frac{1}{2\pi} < \frac{w}{h} < 2$:

$$\alpha_c(\omega) = \frac{1}{2\pi Z_0 h}\left\{1-\left(\frac{w'}{4h}\right)^2\right\}\left\{\left[\frac{R_{s1}+R_{s2}}{2}\right]\left[1-\frac{t}{\pi w'}\right] + R_{s1}\frac{h}{w'}\left[1+\frac{1}{\pi}\ln\left(\frac{2h}{t}\right)\right]\right\} \quad \left(\frac{\text{nepers}}{\text{unit length}}\right) \tag{2b}$$

$\frac{w}{h} \geqslant 2$:

$$\alpha_c(\omega) = \frac{1}{Z_0 h}\left\{\frac{w'}{h}+\frac{2}{\pi}\ln\left[2\pi e\left(\frac{w'}{2h}+0.94\right)\right]\right\}^{-2}\left\{\frac{w'}{h}+\frac{w'/\pi h}{\frac{w'}{2h}+0.94}\right\} \times\left\{\left[\frac{R_{s1}+R_{s2}}{2}\right]\left[1-\frac{t}{\pi w'}\right]+R_{s1}\frac{h}{w'}\left[1+\frac{1}{\pi}\ln\left(\frac{2h}{t}\right)\right]\right\} \quad \left(\frac{\text{nepers}}{\text{unit length}}\right) \tag{2c}$$

where

$$R_{s1} = \sqrt{\pi f \mu_1 \rho_1}, \tag{2d}$$

$$R_{s2} = \sqrt{\pi f \mu_2 \rho_2}, \tag{2e}$$

w width of the strip conductor,
h height of the dielectric substrate,
t thickness of the strip conductor,
Z_0 characteristic impedance of the microstrip line,
$\mu_{1,2}$ permeability of the center strip and ground conductors, respectively,
$\rho_{1,2}$ resistivity of the center strip and ground conductors, respectively,
f frequency in Hz,

and w' is the effective strip width which accounts for the nonzero strip thickness and is given in [8] and [9]. In computing $\alpha_c(\omega)$, the line conductors are assumed to be perfectly smooth with no losses due to surface roughness. Typical values for the surface resistivity are $(2.61\times10^{-7})\sqrt{f}$ for copper and $(3.26\times10^{-7})\sqrt{f}$ for aluminum.

The expression for $\alpha_d(\omega)$ can be written as [7], [10]

$$\alpha_d(\omega) = \pi \frac{\epsilon_r}{\sqrt{\epsilon_{r_{\text{eff}}}(0)}} \cdot \frac{\epsilon_{r_{\text{eff}}}(0) - 1}{\epsilon_r - 1} \frac{\tan\delta}{\lambda_0} \quad \left(\frac{\text{nepers}}{\text{unit length}}\right) \quad (3)$$

where

ϵ_r relative dielectric constant of the substrate,
$\epsilon_{r_{\text{eff}}}(0)$ effective dielectric constant at $f = 0$,
λ_0 free-space wavelength,
$\tan\delta$ loss tangent of the substrate.

The loss tangent here is assumed to be constant with frequency. Typical values of $\tan\delta$ are 0.0015 for 6010 RT/duroid ($\epsilon_r = 10.2$) and 0.0005 for 5870 RT/duroid ($\epsilon_r = 2.33$).

The dispersion distortions of pulses are calculated from Pramanick and Bhartia's model [11] for the effective dielectric constant $\epsilon_{r_{\text{eff}}}(f)$ since rigorous solutions for $\epsilon_{r_{\text{eff}}}(f)$, such as the full-wave analyses [12], [13], require time-consuming computations. In addition, Pramanick and Bhartia's model for $\epsilon_{r_{\text{eff}}}(f)$ is shown to be accurate compared to other quasi-static formulas [1].

The computations for the distorted waveforms at a distance L along a microstrip line are made using [1]

$$V(t, z = L) = \frac{1}{2\pi} \int_{-\infty}^{+\infty} V(\omega, z = 0)\, e^{[j\omega t - \gamma(\omega) L]}\, d\omega \quad (4a)$$

where

$$\gamma(\omega) = \alpha(\omega) + j\beta(\omega) \quad (4b)$$

$$\beta(\omega) = \frac{\omega}{c}\sqrt{\epsilon_{r_{\text{eff}}}(f)} \quad (4c)$$

and $V(\omega, z = 0)$ is the Fourier transform of the pulse at the reference point ($L = 0$) of the line.

III. Numerical Results and Discussion

Fig. 1(a) and (b) shows 20-picosecond-wide (at the half magnitude points) Gaussian pulses propagating on a microstrip line with a strip conductor of copper, a ground plane of aluminum, and a substrate of 6010 RT/duroid. This figure illustrates the changes in distortions (compared to the distortionless pulse) as the strip width is increased from 0.001 in to 0.01 in. The conduction losses become smaller because the current density in the strip conductor decreases as the strip width increases (for a given amount of current). This causes lower ohmic losses. However, the dielectric losses are not changed. In fact, as seen in Figs. 1 and 2, the geometry parameters do not affect the dielectric losses, because (3) is only weakly dependent upon the strip width and substrate height. The dispersion distortions become greater, because a wider strip conductor decreases the inflection frequency of the effective dielectric constant [11], which means that more high-frequency components of the pulse travel with a lower (compared to the low-frequency components) phase velocity [i.e., $v_p = c/\sqrt{\epsilon_{r_{\text{eff}}}(f)}$].

For the pulse distortions exhibited in Fig. 2(a) and (b), the substrate height is changed from 0.004 in to 0.01 in with w remaining constant. Again notice that the conduction losses are diminished and the dispersion distortions are greater. In this case the conduction losses are smaller because Z_0 becomes larger as a function of decreasing w/h [7]. A greater value of Z_0 means that for a given potential between the strip conductor and ground plane, the current flowing along the line (and the ohmic losses) will diminish. The dispersion distortions increase because a larger value for the substrate height also decreases the inflection frequency of the effective dielectric constant (and with results similar to increasing the strip width, as comparing Figs. 1(b) and 2(b) shows).

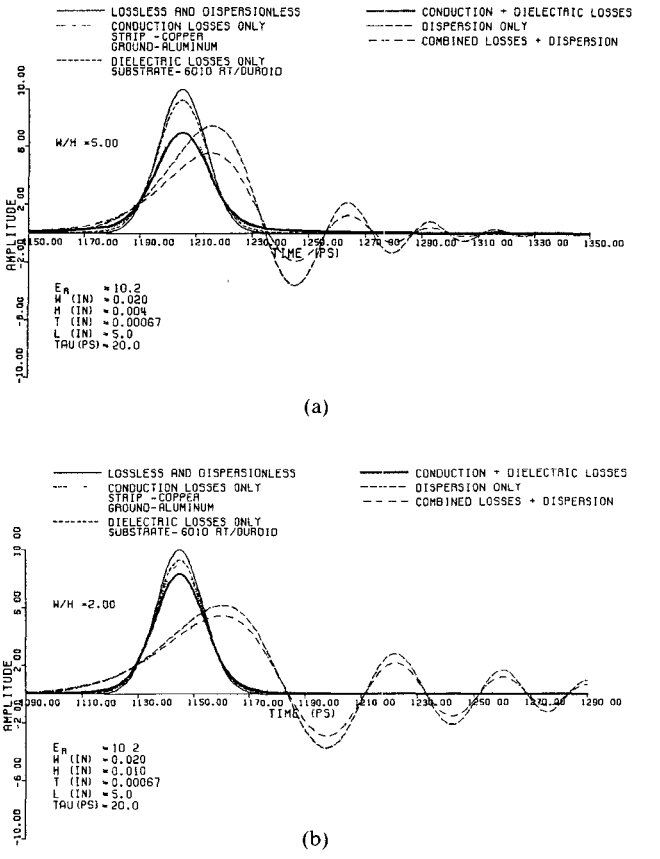

Fig. 2. Gaussian pulse attenuation and dispersion as functions of substrate height at $L = 5$ in (12.7 cm) along a microstrip line.

Fig. 3(a) and (b) displays distorted triangular pulses as the substrate dielectric constant increases from 2.33 to 10.2. Since the two duroid materials have different loss tangents, a $\tan\delta = 0.0015$ was assumed for both so that the effect of changing ϵ_r can be isolated. Note that both types of losses are enhanced. The conduction loss increase is explained by the fact that Z_0 decreases monotonically as a function of increasing ϵ_r, causing the strip current and ohmic losses to become larger in magnitude. The dielectric losses increase because a larger ϵ_r confines more of the electric field lines (from the strip conductor to the ground plane) to the substrate. This greater confinement intensifies the field strength within the substrate, which in turn causes more dissipation of the electric field energy of the pulse. A larger ϵ_r also increases dispersion distortions, an effect that again involves the electric field lines. These fields become more discontinuous as ϵ_r increases, giving rise to a greater number of surface waves propagating along the microstrip line. These surface waves cause the effective dielectric constant, and the phase velocity, to become more nonlinear.

The effects of changing the pulse width and the pulse rise time are approximately the same. Fig. 4(a) and (b) shows a decrease in the square pulse width (from 20 to 10 picoseconds) while Fig. 5(a) and (b) shows a change from a Gaussian to a stepped-square pulse. In Fig. 4(a) and (b) the conduction and dielectric losses, as well as dispersion distortions, are enhanced. The increase in dispersion distortions here is seen as a drop in magnitude of the first peak of the dispersed pulse (from part (a) to part (b)). In Fig. 5(a) and (b) the stepped-square pulses (compared to the Gaussian pulses) show a slight increase in both types of losses.

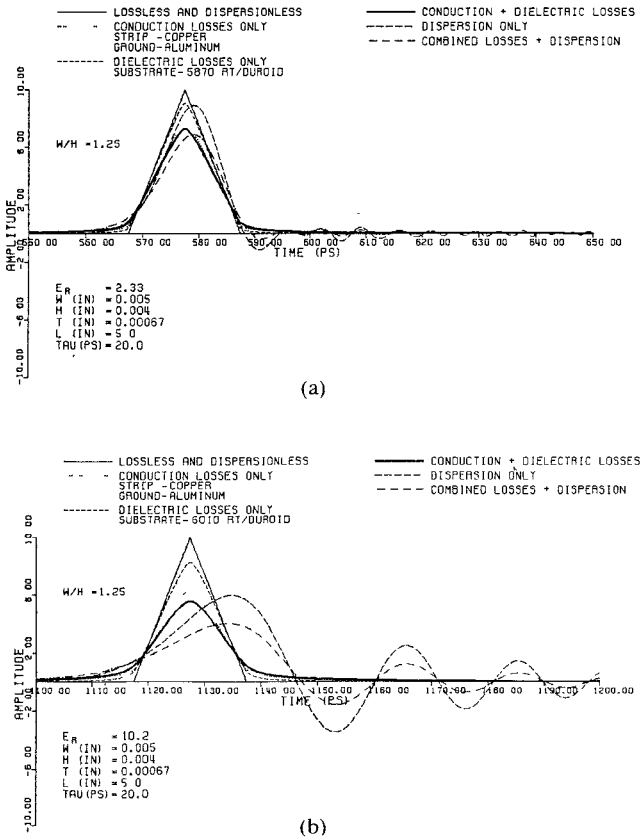

Fig. 3. Triangular pulse attenuation and dispersion as functions of substrate dielectric constant.

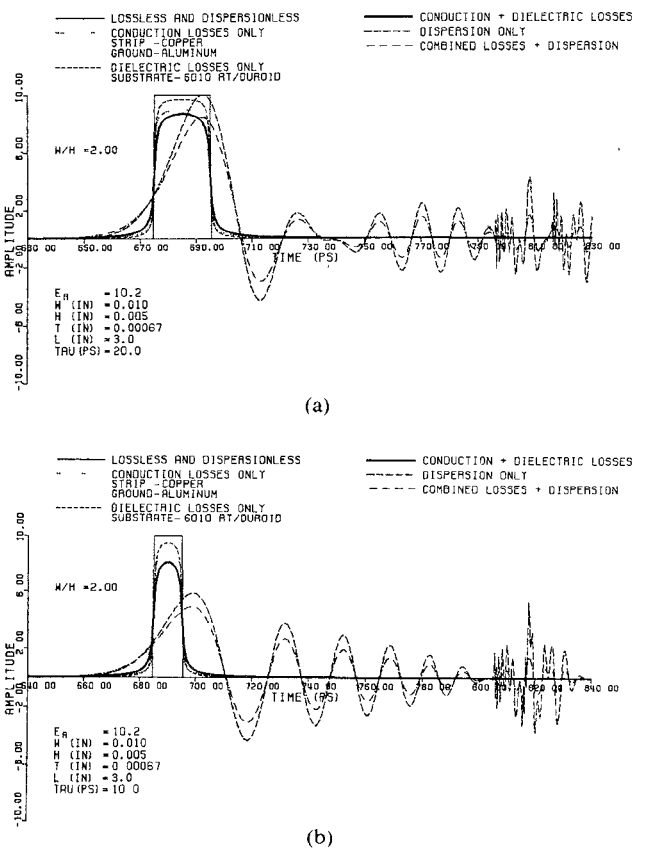

Fig. 4. Square pulse attenuation and dispersion as functions of pulse width at $L = 3$ in (7.62 cm) along a microstrip line

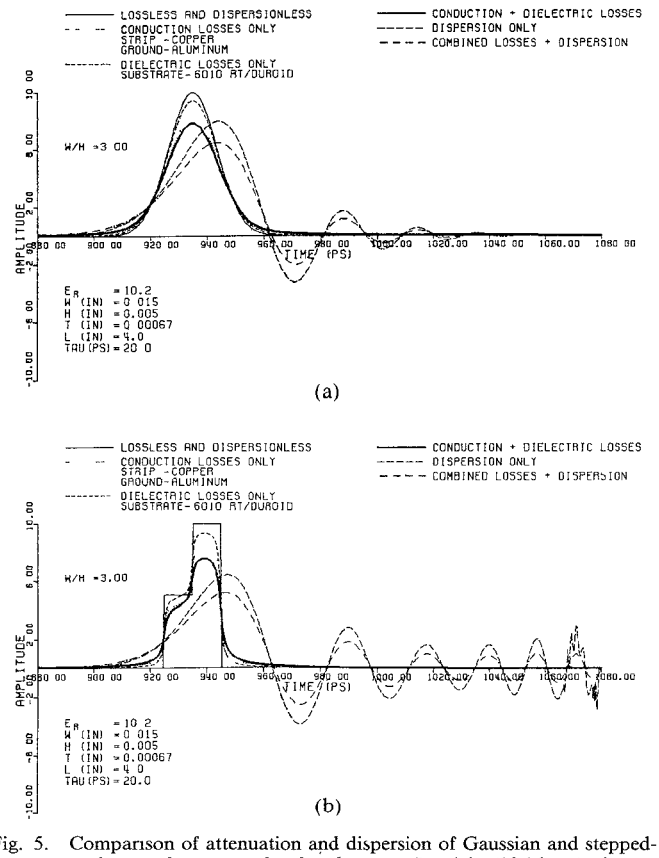

Fig. 5. Comparison of attenuation and dispersion of Gaussian and stepped-square pulses as functions of pulse shape at $L = 4$ in (10.16 cm) along a microstrip line.

The dispersion distortions, however, are much more pronounced in the stepped-square pulse. In both figures here the bandwidth of the transient signal is increased. Since the conduction and dielectric loss constants increase monotonically as a function of increasing frequency, it is clear that a wider bandwidth means more high-frequency components being attenuated and, subsequently, more total losses. A wider bandwidth also means that more high-frequency components having different phase velocities (than the low-frequency components) are present, which creates a more dispersed pulse.

IV. Conclusions

Attenuation and dispersion distortions of short electric pulses are examined for microstrip lines. Conduction and dielectric losses were considered for microstrip lines with common isotropic substrates and with different resistivities for the strip conductor and the ground plane. Results show that attenuation and dispersion distortions change (from the distortionless pulse) by varying the strip width, substrate height, substrate dielectric constant, pulse width, and pulse rise time.

Acknowledgment

The authors would like to thank Dr. J. W. Mink of the Electronics Division, Army Research Office, for his interest and support of the project, and T. Griesser for the expert typing of the manuscript.

References

[1] R. L Veghte and C. A Balanis, "Dispersion of transient signals in microstrip transmission lines," *IEEE Trans. Microwave Theory Tech.*, vol MTT-34, pp. 1427-1436, Dec. 1986.

[2] R. L. Veghte and C. A. Balanis, "Dispersion of transient signals in microstrip transmission lines," in *1986 IEEE MTT-S Int. Microwave Symp. Dig.* (Baltimore, MD), June 2–4, 1986, pp. 691–694.
[3] K. K. Li *et al.*, "Propagation of picosecond pulses on microwave striplines," *IEEE Trans. Microwave Theory Tech.*, vol. MTT-30, pp. 1270–1273, Aug. 1982.
[4] M. P. Forrer, "Analysis of millimicrosend RF pulse transmission," *Proc. IRE*, vol. 46, pp. 1830–1835, Nov. 1958.
[5] R. D. Wanselow, "Rectangular pulse distortion due to a nonlinear complex transmission propagation constant," *J. Franklin Inst.*, vol. 274, pp. 178–184, Sept. 1962
[6] E. Belohoubek and E. Denlinger, "Loss considerations for microstrip resonators," *IEEE Trans. Microwave Theory Tech.*, vol. MTT-23, pp. 522–526, June 1975.
[7] I. J. Bahl and D. K. Trivedi, "A designer's guide to microstrip," *Microwaves*, vol. 16, no. 5, pp. 174–182, May 1977.
[8] R. A. Pucel, D. J. Massé, and C. P. Hartwig, "Losses in microstrip," *IEEE Trans. Microwave Theory Tech.*, vol. MTT-16, pp 342–350, June 1968.
[9] R. A. Pucel, D. J. Massé, and C. P Hartwig, "Correction to 'Losses in microstrip'," *IEEE Trans Microwave Theory Tech.*, vol. MTT-16, p. 1064, Dec. 1968.
[10] M. V. Schneider, "Dielectric loss in integrated microwave circuits," *Bell Syst. Tech. J.*, vol. 48, no. 7, pp. 2325–2332, Sept. 1969.
[11] P. Pramanick and P. Bhartia, "An accurate description of dispersion in microstrip," *Microwave J.*, vol. 26, no. 12, pp. 89–96, Dec. 1983.
[12] R. Mittra and T. Itoh, "A new technique for the analysis of the dispersion characteristics of microstrip lines," *IEEE Trans. Microwave Theory Tech.*, vol. MTT-19, pp. 47–56, Jan. 1971.
[13] T. Itoh and R. Mittra, "Spectral-domain approach for calculating the dispersion characteristics of microstrip lines," *IEEE Trans. Microwave Theory Tech.*, vol. MTT-21, pp. 496–499, July 1973.

A Spectral Iterative Technique with Gram–Schmidt Orthogonalization

PETER M. VAN DEN BERG AND WALTER J. GHIJSEN

Abstract — **Iterative schemes based on the minimization of the integrated square error are discussed. In each iteration a basis function is generated in such a way that it is linearly related to the residual error of the previous iteration. A complete orthogonalization of all of these basis functions leads to an optimal convergent scheme for some choices of the basis functions. In order to reduce the computer storage needed to store all of the basis functions, we present an incomplete orthogonalization scheme that still yields an efficient computational method. In this scheme a limited number of basis functions has to be stored. Some numerical results with respect to some representative field problems illustrate the performance of the various versions of the iterative schemes suggested here.**

I. Introduction

The spectral iterative technique (SIT), developed by Bojarski [1] and Ko and Mittra [2], has been applied to a wide class of radiation and scattering problems. Convergence problems arising in the spectral iterative technique, which are serious at times, have been eliminated by van den Berg [3] by minimizing the integrated square error in the boundary conditions on the pertinent radiating or scattering object. The convergence has substantially been improved by using all available functions of the previous iteration in the minimization procedure of each iteration (CST3-scheme [4]). In each iteration of the iterative schemes a basis function is generated in such a way that it is linearly related to the residual error of the previous iteration. MacKay and McCowen [5] have suggested a full orthogonalization of all basis functions in order to improve the convergence in an optimum way. This requires all basis functions to be stored in the computer; hence sufficient computer memory must be available. The latter authors therefore suggest that a complete orthogonalization may not be necessary and that the number of basis functions to be orthogonalized can be limited to a small number. However, in this case, the convergence can decrease dramatically after a number of iterations.

In the present paper we discuss an incomplete orthogonalization scheme where we take into account a limited number of basis functions generated in the last few iterations; however, in contrast to [5], we also use the appropriate estimate of one of the previous iterations as a function to which all the relevant basis functions have to be orthogonalized. This maintains the speed of convergence. Further, in one of the most simple forms, the latter scheme turns out to be equivalent to the contrast-source-truncation technique CST3 [4]. The latter is a truly iterative technique, because it needs the functions of the previous iteration only.

II. The Operator Equation

We consider a field computation problem in terms of an integral equation of the form [4]

$$\int_D K(x-x')f(x')\,dx' = g(x), \qquad \text{when } x \in D \tag{1}$$

where D is the domain of observation. Then, (1) is equivalent to

$$Kf = g, \qquad \text{when } x \in D. \tag{2}$$

Further, we introduce the inner product of two functions f and g as (the bar denotes a complex conjugate)

$$\langle f, g\rangle = \int_D \overline{f(x)}g(x)\,dx \tag{3}$$

while the norm of a function f is defined as $\|f\| = \langle f, f\rangle^{1/2}$. We further introduce the characteristic function $\chi_D(x) = 1$ when $x \in D$, and $\chi_D(x) = 0$ when $x \in D'$, where D' is the subdomain outside the domain D of observation.

Introducing the spatial Fourier transform of a function f as $\tilde{f} = F\{f\}$, the Fourier transform of the operator expression Kf of (2) can be written as the product of the Fourier transforms $\tilde{K} = F\{K(x)\}$ and $F\{\chi_D f\}$; thus the operator expression can be written as

$$Kf = F^{-1}\{\tilde{K}F\{\chi_D f\}\}. \tag{4}$$

III. Iterative Approximation with Gram–Schmidt Orthogonalization

In our iterative approximation we construct a sequence of functions $\{f_n,\ n = 0,1,2,3,\cdots\}$ such that the norm of the residual in the operator eq. (2),

$$ERR_n = \langle r_n, r_n\rangle^{1/2}, \qquad \text{with } r_n = Kf_n - g \tag{5}$$

decreases with increasing n in an optimum way. The procedure starts with an initial guess f_0 with the associated residual r_0. At each step of the iterative procedure, we write

$$f_n = f_{n-1} + \alpha_n f_n^c, \qquad n = 1,2,3,\cdots \tag{6}$$

where, in each step, f_n^c is a correction function and where the complex parameter α_n is chosen such that the error ERR_n is

Manuscript received May 4, 1987; revised October 14, 1987.
P. M. van den Berg is with the Laboratory of Electromagnetic Research, Department of Electrical Engineering, Delft University of Technology, P.O Box 5031, 2600 GA Delft, The Netherlands.
W. J. Ghijsen was with the Department of Electrical Engineering, Delft University of Technology, Delft, The Netherlands. he is now with Phonon, Inc., Simsbury CT 06070.
IEEE Log Number 8719204.

0018-9480/88/0400-0769$01.00 ©1988 IEEE